



POLİTEKNİK DERGİSİ

*JOURNAL of POLYTECHNIC*

ISSN: 1302-0900 (PRINT), ISSN: 2147-9429 (ONLINE)

URL: <http://dergipark.org.tr/politeknik>



# Numerical comparison of turbulence models for a NACA 0012 aerofoil with gurney flap

*Gurney flaplı NACA 0012 kanat profili için türbülans modellerinin sayısal karşılaştırılması*

Yazar(lar) (Author(s)): Gökhan ÇAL<sup>1</sup>, Halit ARAT<sup>2</sup>

ORCID<sup>1</sup>: 0000-0002-8451-9808

ORCID<sup>2</sup>: 0000-0002-6634-2535

**To cite to this article:** Çal G., and Arat H., “Numerical Comparison of Turbulence Models for a NACA 0012 Aerofoil with Gurney Flap”, *Journal of Polytechnic*, 29(4):290434:1-10 (2026).

**Bu makaleye şu şekilde atıfta bulunabilirsiniz:** Çal G. ve Arat H., “Numerical Comparison of Turbulence Models for a NACA 0012 Aerofoil with Gurney Flap”, *Politeknik Dergisi*, 29(4):290434:1-10 (2026).

**Erişim linki (To link to this article):** <http://dergipark.org.tr/politeknik/archive>

**DOI:** 10.2339/politeknik.1699998

# Numerical Comparison of Turbulence Models for a NACA 0012 Aerofoil With Gurney Flap

## Highlights

- ❖ Five turbulence models were compared using CFD on a NACA 0012 aerofoil with a 1.5% Gurney flap.
- ❖ Simulations were performed at angles of attack of  $0^\circ$  to  $12^\circ$ .
- ❖  $k-\epsilon$  Realizable model achieved the highest  $CL/CD$  ratio at  $\alpha = 8^\circ$  according to the best aerodynamic performance.
- ❖ The Realizable  $k-\epsilon$  model demonstrated superior consistency in predicting lift enhancement and separation behavior.

## Graphical Abstract

The figure below shows the variation of  $CL/CD$  with angle of attack for five different turbulence models. It is demonstrated that the Transition SST model provides the highest aerodynamic efficiency from  $0^\circ$  to  $4^\circ$  while  $k-\epsilon$  Realizable model gives the best of that after  $6^\circ$  until  $12^\circ$ .

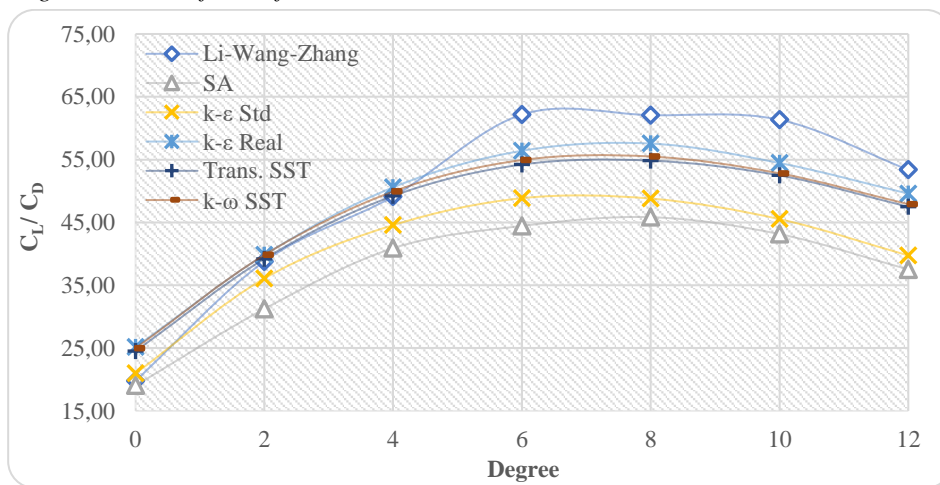


Figure. Lift-to-drag ratio ( $C_L/C_D$ ) vs. angle of attack for different turbulence models.

## Aim

This study aims to numerically investigate the aerodynamic performance of a NACA 0012 airfoil equipped with a 1.5% Gurney flap. The objective is to determine the most suitable turbulence model by evaluating lift, drag, and  $C_L/C_D$  ratio variations.

## Design & Methodology

The numerical simulations were performed in two dimensions using ANSYS Fluent. Five different turbulence models were compared under identical mesh and boundary conditions.

## Originality

Unlike previous research, this study compares five turbulence models under identical mesh and boundary conditions, revealing that the  $k-\epsilon$  Realizable model provides superior predictive capability for configurations using passive flow control.

## Findings

$k-\epsilon$  Realizable consistently showed the highest agreement with experimental results and predicted maximum aerodynamic efficiency at  $\alpha = 8^\circ$ , with the best  $CL/CD$  ratio among the models evaluated.

## Conclusion

The results suggest that the Transition SST and  $k-\epsilon$  Realizable models are the most reliable for simulating airfoils equipped with Gurney flaps, especially for transitional flow regimes. It is recommended for future CFD studies focused on aerodynamic optimization.

## Declaration of Ethical Standards

The authors declare that this computational study does not require ethical committee approval or special permissions.

# Numerical Comparison of Turbulence Models For a Naca 0012 Aerofoil With Gurney Flap

*Araştırma Makalesi / Research Article*

Gökhan ÇAL<sup>1\*</sup>, Halit ARAT<sup>2</sup>

<sup>1</sup>Kütahya Dumlupınar University, Institute of Graduate Education, Department of Mechanical Engineering, Kütahya, Turkey

<sup>2</sup>Kütahya Dumlupınar University, Faculty of Engineering, Department of Mechanical Engineering, Kütahya, Turkey

(Geliş/Received : 15.05.2025 ; Kabul/Accepted : 17.12.2025 ; Erken Görünüm/Early View : 03.01.2026)

## ABSTRACT

This study presents a computational investigation on the aerodynamic behavior of a NACA 0012 aerofoil equipped with a 1.5% height Gurney flap, utilizing various turbulence models in ANSYS Fluent. Five widely recognized turbulence models—Spalart-Allmaras, Standard k- $\epsilon$ , Realizable k- $\epsilon$ , SST k- $\omega$ , and Transition SST—were employed to assess their predictive accuracy under identical flow conditions. The primary objective was to determine the most appropriate model to capture the aerodynamic effects caused by the trailing-edge Gurney flap, particularly in terms of lift coefficient, drag coefficient, and lift-to-drag ratio. A mesh independence study was conducted to ensure numerical reliability, and the results were interpreted considering prior studies that investigated Gurney flap performance on symmetric airfoils. According to results, it is demonstrated that the Transition SST model provides the highest aerodynamic efficiency from 0° to 4° while k- $\epsilon$  Realizable model gives the best of that after 6° until 12°. Among the models investigated, the k- $\epsilon$  Realizable model exhibited superior consistency in predicting both lift enhancement and flow separation behavior. The findings reveal that the k- $\epsilon$  Realizable model, which yields the highest lift-to-drag ratio ( $C_L/C_D$ ) particularly at an angle of attack of  $\alpha = 8^\circ$ , is the most suitable turbulence model for CFD-based aerodynamic optimization studies involving passive flow control devices such as Gurney flaps. In this context, this study provides an important perspective on turbulence model selection for low Reynolds number applications.

**Keywords:** NACA 0012, Gurney flap, CFD, Turbulence Modeling, Lift-to-Drag Ratio

## Gurney Flaplı Naca 0012 Kanat Profili için Türbülans Modellerinin Sayısal Karşılaştırılması

### ÖZ

Bu çalışma, fırac kenarına %1.5c yüksekliğinde Gurney flap entegre edilmiş NACA 0012 kanat profilinin aerodinamik davranışını, farklı türbülans modelleri kullanılarak gerçekleştirilen sayısal analiz yoluyla incelemektedir. ANSYS Fluent yazılımı kullanılarak, Spalart-Allmaras, Standard k- $\epsilon$ , Realizable k- $\epsilon$ , SST k- $\omega$  ve Transition SST olmak üzere beş farklı türbülans modeli, aynı akış koşulları altında aerodinamik performansın öngörülmesindeki başarıları açısından karşılaştırılmıştır. Bu çalışmanın temel amacı, Gurney flap uygulamasının kaldırma kuvveti katsayısı, sürüklenme katsayısı ve kaldırma/sürüklenme oranı üzerindeki etkilerini doğru şekilde tahmin edebilen en uygun türbülans modelini belirlemektir. Sayısal güvenilirliğin sağlanması amacıyla ağdan bağımsızlık (mesh independence) çalışması gerçekleştirilmiş ve elde edilen sonuçlar, simetrik kanat profilleri üzerinde yapılan önceki Gurney flap araştırmaları ile karşılaştırılarak değerlendirilmiştir. Sonuçlar incelendiğinde, Transition SST modelinin 0°'den 4°'ye kadar en yüksek aerodinamik verimliliği sağladığı, k- $\epsilon$  Realizable modelinin ise 6°'den 12°'ye kadar en iyi aerodinamik verimliliği sağladığı ortaya konulmuştur. Ele alınan modeller arasında, k- $\epsilon$  Realizable modeli hem kaldırma kuvveti artışı hem de ayrılma bölgesi öngörüsünde en tutarlı sonuçları vermiştir. Elde edilen bulgular, özellikle  $\alpha = 8^\circ$  hücum açısında en yüksek kaldırma/sürüklenme oranını ( $C_L / C_D$ ) sağlayan k- $\epsilon$  Realizable modelinin, Gurney flap gibi pasif akış kontrol elemanlarını içeren CFD tabanlı aerodinamik optimizasyon çalışmaları için en uygun türbülans modeli olduğunu ortaya koymaktadır. Bu bağlamda, düşük Reynolds sayılı uygulamalarda türbülans modeli seçimine yönelik önemli bir içgörü sunmaktadır.

**Anahtar Kelimeler:** NACA 0012, Gurney flap, Hesaplamalı Akışkanlar Dinamiği (HAD), Türbülans Modellemesi, Kaldırma/Sürüklenme Oranı

## 1. INTRODUCTION

In recent years, studies on analyzing and improving the aerodynamic performance of airfoils used in various engineering applications such as aircraft, unmanned aerial vehicles (UAVs) and wind turbines have increased. In analyzing this performance, optimization of lift ( $C_L$ ) and drag ( $C_D$ ) coefficients directly contributes to improving fuel efficiency, extending operational range and increasing payload capacity [1]. Besides at low Reynolds numbers, which are often seen in UAVs and

small-scale systems, accurately predicting flow separation and transition becomes particularly difficult and requires advanced aerodynamic modeling [2].

To overcome these challenges, one effective solution is to use passive flow control devices such as Gurney flaps. These small flaps are mounted vertically on the trailing edge of the airfoil, creating counter-rotating vortices that improve circulation and increase lift, thus modifying the flow behavior [3]. The effectiveness of Gurney flaps becomes more pronounced at high angles of attack and low speeds. However, this increase in lift generally

\*Sorumlu Yazar (Corresponding Author)  
e-posta : gokhan\_cal1001@hotmail.com

produces an increase in aerodynamic drag, which depends largely on the height, angle, and location of the flaps [4].

Successful agreement between numerical simulations incorporating flow control devices and real-world values depends largely on the choice of turbulence model. Reynolds-averaged Navier-Stokes (RANS) models, commonly used in the literature, are computationally efficient, although they differ in their handling of boundary layer separation, adverse pressure gradients, and wake structures [5]. Therefore, selecting an appropriate turbulence model that satisfies the desired condition is crucial for the accuracy and reliability of numerical results. In this direction, different turbulence models such as Spalart-Allmaras, standard and realizable  $k-\varepsilon$ ,  $k-\omega$  SST and SST transition models have been frequently evaluated for airfoil simulations in the literature [6].

CFD studies have been widely used in the literature for different wing profiles because they provide the opportunity to perform numerous analyses inexpensively [7-9]. Karthikeyan and Harish conducted CFD on a cambered NACA 4412 airfoil with Gurney flaps and showed that the flap mounting orientation affects  $C_L/C_D$ ; a nearly normal ( $\approx 90^\circ$ ) tab is the conventional implementation, and orientation changes can produce measurable shifts in efficiency for a given flap height and Reynolds-number range [10]. Evran and Yıldır combined CFD with a Taguchi design for NACA 0009 and NACA 4415 and reported that both  $C_L$  and  $C_D$  are highly sensitive to the angle of attack, underscoring the need for consistent model and mesh settings in low-Re comparisons [11]. Also, Gökçe et al. have used CFD to computationally investigate the effects of curvature and area distribution on the performance of an S-shaped subsonic diffuser, as well as the dependence of different parameters on the centerline curvature and area ratio for each flight condition. Their study demonstrated that low distortion can be achieved with high curvature at the diffuser inlet and a uniform field increase along the channel [12].

On the other hand, some studies have been focused on the situation of low Reynolds number. A comparative study on NACA 0012 at low-to-moderate Reynolds numbers reported that the  $k-\omega$  SST model provided the most consistent  $C_L - C_D$  trends within the tested conditions, highlighting its robustness in separated/adverse-pressure-gradient flows [13]. Durmuş and Ulutaş performed a numerical analysis of the Eppler 423 and NACA 6409 airfoils and discussed how lift and drag characteristics vary with angle of attack at low Reynolds numbers, emphasizing the role of transition and near-wall resolution in credible predictions [14].

While comparing RANS models on the NACA 0012 airfoil with Gurney vanes with Celik's study on near-wall operation and separated flow behavior, we target  $y^+ \approx 1$  and address the boundary layer [15]. Besides, these correlation-based  $\gamma-Re_\theta$  transition model by Langtry and

Menter augments RANS with local transport equations to predict laminar-turbulent transition; here its Transition SST formulation was used to capture separation-induced transition at low Reynolds numbers [16]. The performance of a NACA 0009 airfoil at low Reynolds numbers was analyzed, and an angle of attack of about  $5^\circ$  has been identified as yielding the peak  $C_L/C_D$  within the tested conditions [17]. Moreover, some studies on several four-digit NACA sections have reported cases where increasing airfoil thickness is associated with a reduction in the attainable lift (e.g., lower  $C_{L,max}$  and earlier stall); however, the trend is Reynolds-number and geometry dependent, which is important when assessing Gurney-flap performance [18].

Coupled aerodynamic-structural analysis comparing a free-form wing design to a NACA 0012 section found that, for the studied configuration, positive angles of attack led to higher stress and deformation due to asymmetric flow distribution [19]. On bare NACA 0012 at low Reynolds number ( $Re \approx 5.1 \times 10^4$ ), a comparative CFD study evaluated Spalart-Allmaras,  $k-\varepsilon$ ,  $k-\omega$ , and Transition SST at  $\alpha = 0^\circ, 5^\circ, 10^\circ$ , and  $15^\circ$ , reporting model-dependent differences in separation and forces;  $k-\omega$  matched  $C_L$  and  $C_D$  trends best at moderate angles, while Transition SST yielded steadier post-stall  $C_L$  [20]. In the Gurney-flapped NACA 0012 cases, different turbulence models were highlighted for low Re, near-stall conditions due to trend fidelity  $C_L$  and  $C_D$  [21].

In this study, a computational investigation on the aerodynamic behavior of a NACA 0012 airfoil equipped with a 1.5% height Gurney flap was performed by utilizing various turbulence models in ANSYS Fluent. For this purpose, different five widely recognized turbulence models -Spalart-Allmaras, Standard  $k-\varepsilon$ , Realizable  $k-\varepsilon$ , SST  $k-\omega$ , and Transition SST- were employed to assess their predictive accuracy under identical flow conditions.

## 2. MATERIAL and METHOD

This section presents the computational setup and modeling strategies adopted to analyze the aerodynamic performance of a NACA 0012 aerofoil equipped with a Gurney flap. The methodology includes the geometric configuration, computational domain, mesh generation, turbulence models applied, and boundary conditions used in the simulations.

### 2.1. Airfoil and Gurney Flap Geometry

The aerofoil used in the analysis is the symmetric NACA 0012 profile. In all simulations, the chord length was normalized to unity (1.0). A fixed Gurney flap with a height of 1.5% of the chord length (1.5% $c$ ) was mounted vertically at the trailing edge. In this study, the Gurney flap height was fixed at 1.5% $c$  for the NACA 0012 model because it provides a stable operating point at low to moderate Reynolds numbers. Literature studies indicate that heights in the range of 1–2% $c$  around this profile provide a significant increase in lift and generally modest drag [3]. Therefore, 1.5% $c$  enhances the pre-stall

circulation and delays separation at the studied angles of attack. However, as a moderate height that does not cause excessive vortex shedding, this value provides a turbulence model comparison without biasing the flap to favor either a too weak ( $\leq 1c$ ) or an overly aggressive ( $\geq 2-3c$ ) flap. Furthermore, this value is consistent with previous applications on the NACA 0012 model, facilitating direct comparison of the CL, CD, and CL/CD trends with published results. Figure 1 shows the two-dimensional representation of this flap-integrated configuration.

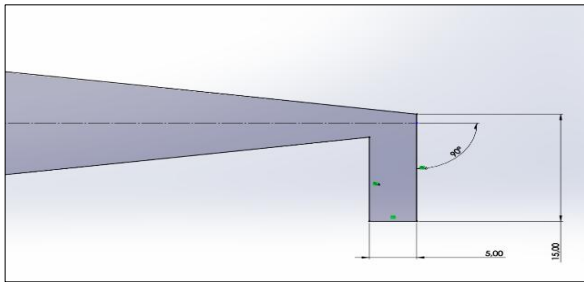


**Figure 1.** NACA 0012 airfoil with 1.5% c Gurney flap

**2.2. Computational Domain and Boundary Conditions**

A two-dimensional computational domain was constructed to simulate the external flow over the NACA 0012 airfoil with a Gurney flap. As shown in Figure 2, the domain had a total length and height of 15,000 units, with the airfoil placed 1,000 units downstream from the semi-circular inlet. The trailing edge of the airfoil was located approximately at the center of the domain.

The curved inlet section allowed for a uniform and smooth inflow profile, minimizing upstream disturbances. The outlet was placed far enough downstream to ensure wake development without numerical interference. The top and bottom boundaries were located at equal distances from the airfoil centerline to maintain geometric symmetry.

Boundary conditions were defined as follows: velocity inlet at the left semi-circular arc, pressure outlet at the right boundary, symmetry at the top and bottom, and no-slip condition on the airfoil surface.

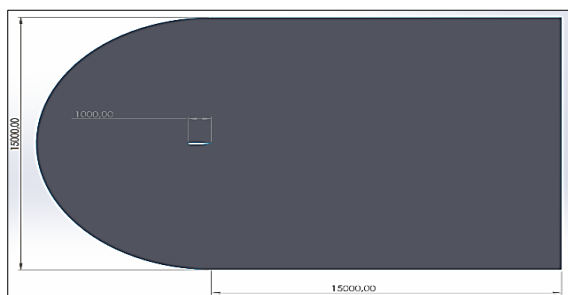


**Figure 2.** 2D computational domain for the NACA 0012 airfoil with a Gurney flap

**2.3. Mesh Structure and Grid Independence Study**

A hybrid mesh consisting of structured and unstructured elements has been generated around the NACA 0012

airfoil with a 1.5% c Gurney flap. As shown in Figure 3, a high-density mesh was applied near the trailing edge and flap region to resolve steep pressure gradients and vortex shedding more accurately. The mesh was gradually coarsened toward the far-field boundaries to reduce computational cost while maintaining simulation accuracy. The final mesh quality was evaluated based on multiple criteria, including aspect ratio, element quality, orthogonal quality, and skewness.

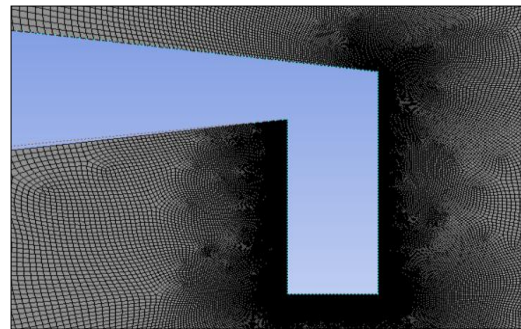


**Figure 3.** Locally refined mesh around the NACA 0012 airfoil with Gurney flap

The mesh demonstrated a minimum skewness of 0.0000637, an average of 0.1518, and a maximum of 0.7010, all of which fall within acceptable limits for RANS-based CFD simulations. Orthogonal quality ranged from 0.5212 to 1.0000, with an average value of 0.9669, indicating well-formed cells in critical flow regions. Additional mesh quality metrics are summarized in Table 1. To ensure mesh-independent results, a grid convergence study was conducted by evaluating the lift-to-drag ratio (CL/CD) across different mesh densities ranging from 40,000 to 120,000 cells, using various turbulence models. As shown in Figure 4, CL/CD values exhibited minimal variation beyond 40,000 cells, particularly for the k-ε Realizable model.

Therefore, a mesh with 40,000 elements was adopted for subsequent CFD simulations to maintain a balance between computational cost and accuracy.

**Table 1.** Minimum, average, and maximum values of mesh quality metrics used in the final grid

	Minimum	Average	Maximum
<b>Aspect Ratio</b>	1.00	1.2464	4.2645
<b>Element Quality</b>	0.2985	0.8519	0.9996
<b>Orthogonal Quality</b>	0.5212	0.9669	1.00
<b>Skewness</b>	0.000063	0.1518	0.7010

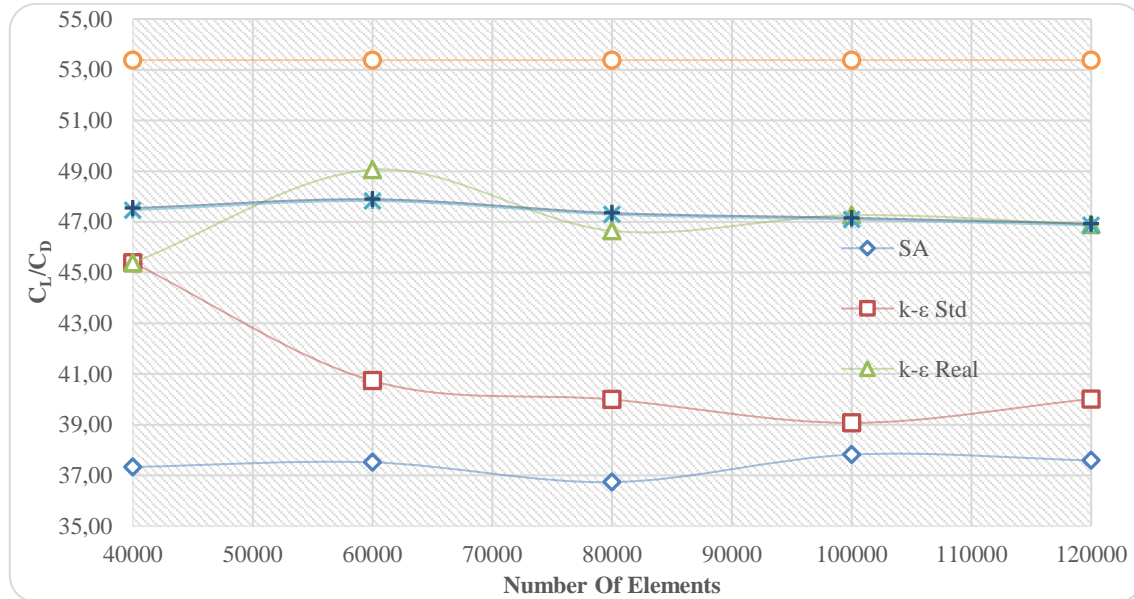


Figure 4. Mesh size effect on lift-to-drag ratio ( $C_L/C_D$ ) for the turbulence models at  $\alpha = 12^\circ$ .

## 2.4. Turbulence Models

The aerodynamic performance of a NACA 0012 airfoil fitted with a 1.5%*c* Gurney flap were assessed by using five RANS turbulence models. The selection of that has focused on differences in near-wall treatment, separation behavior, and transition relevance at low *Re*, as emphasized in aerodynamics studies and NACA 0012 comparisons [5, 13, 22].

Spalart–Allmaras (SA) is a single-equation eddy-viscosity model developed for aerodynamic applications; it is computationally light and reliable for attached boundary layers, though accuracy can drop once separation becomes pronounced [23]. Standard *k*– $\epsilon$  solves two transport equations for turbulent kinetic energy *k* and dissipation rate  $\epsilon$ ; it remains a robust industrial workhorse but is less accurate very close to the wall and tends to underperform under strong adverse-pressure-gradient flows [5], [15]. Realizable *k*– $\epsilon$  modifies the eddy-viscosity relation and the  $\epsilon$  equation, often improving predictions in complex or separated flows relative to the standard formulation [15]. SST *k*– $\omega$  blends *k*– $\epsilon$  away from the wall with *k*– $\omega$  near the wall via zonal weighting, typically sharpening near-wall gradients and separation prediction—especially under adverse-pressure-gradient conditions—and showing competitive trends on NACA 0012 at low-to-moderate *Re* [13], [20]. Transition SST extends SST *k*– $\omega$  with local transport equations for intermittency and transition onset, enabling RANS to capture laminar-to-turbulent transition, which is essential for low-*Re* and stall-proximal analyses [23].

All models have been evaluated on the same mesh with identical boundary conditions and a consistent near-wall treatment to keep the comparison fair. This like-for-like setup allows differences in *CL*, *CD* and overall efficiency to be attributed to the turbulence closure itself rather than numerical choices.

## 2.5. Numerical Setup

CFD simulations presented in this study were performed using the commercial solver ANSYS Fluent. A pressure-based algorithm was utilized under steady-state flow conditions, with the absolute velocity formulation selected for consistency in momentum calculations. The working fluid was defined as air, modeled as an incompressible medium with constant thermophysical properties: a density of 1.225 kg/m<sup>3</sup> and a dynamic viscosity of  $1.7894 \times 10^{-5}$  kg/(m·s). Thermal effects are excluded from the energy equation governing system of equations because they are not relevant to the aerodynamic objectives of the analysis.

Pressure–velocity coupling was handled using the SIMPLE (Semi-Implicit Method for Pressure-Linked Equations) algorithm. To enhance solution accuracy, second-order upwind discretization schemes were applied to all transport equations, including those for momentum, turbulent kinetic energy, and turbulence dissipation (or specific dissipation rate in the case of *k*– $\omega$  models). Pressure interpolation was carried out using the standard discretization scheme, ensuring numerical stability throughout the solution domain.

Boundary conditions and physical parameters for CFD simulations are given in Table 2. Also, a convergence criterion of  $1 \times 10^{-6}$  was applied to all residuals except for continuity, which used a tighter limit of  $1 \times 10^{-7}$  to ensure accurate pressure field prediction. Each turbulence model was run using identical solver settings and boundary conditions for consistency. In all simulations, a no-slip condition was applied at the airfoil surface, and the inlet velocity was set according to the Reynolds number of  $2.1 \times 10^6$ , computed using the unit chord length and corresponding freestream velocity. For near-wall modeling, the enhanced wall treatment approach was applied for the *k*– $\epsilon$  Realizable model, while low-*Re* corrections were only activated for models that require

integration to the wall. Each simulation was iterated until residuals flattened and aerodynamic coefficients stabilized, typically requiring 800–1200 iterations depending on the turbulence model.

**Table 2.** Boundary conditions and physical parameters for CFD simulations.

Boundary Condition	Type	Value / Definition	Description
<b>Inlet</b>	Velocity Inlet	$U=0.7449\text{ m/s}$ $V_x=U\cdot\cos(\alpha), V_y=U\cdot\sin(\alpha)$	Velocity and angle were determined via components.
<b>Outlet</b>	Pressure Outlet	0 Pa Gauge Pressure	Atmospheric pressure at the outlet
<b>Airfoil Surface</b>	Wall (No-slip)	No-slip boundary condition	Zero velocity at the wall surface
<b>Working Fluid</b>	Air (Fluid)	$\rho=1.225\text{kg/m}^3,$ $\mu=1.7894\times 10^{-5}\text{ Pa}\cdot\text{s}$	Standard atmospheric air properties
<b>Flow Regime</b>	Steady, Turbulent	SA, k-ε Std., k-ε Real., k-ω SST, Trans. SST	RANS-based steady state CFD analysis
<b>Angle of Attack</b>	Given via inlet	$\alpha = 0^\circ, 5^\circ, 10^\circ, 15^\circ$	Implemented by adjusting $V_x$ and $V_y$

**3. RESULTS AND DISCUSSION**

This section presents the numerical findings obtained from the CFD analyses of the NACA 0012 airfoil with a 1.5%*c* Gurney flap. Five turbulence models were employed under the identical mesh and boundary conditions. The outcomes include flow visualizations and the variations in aerodynamic coefficients as a function of angle of attack.

**3.1. Pressure and Velocity Distributions**

Velocity contours were generated at angles of 0°, 4°, 8°, and 12° using the k-ε Realizable model. Figure 5 illustrates the flow field around the airfoil. At α = 0°, the low remains symmetric with minor wake formation behind the flap. As α increases to 4° and 8°, velocity intensifies on the upper surface, and a wake region becomes more prominent.

At α = 12°, signs of flow separation near the trailing edge are observable. Figure 6 shows static pressure contours for the same angles. With increasing angle of attack, a distinct low-pressure region forms on the upper surface and becomes more pronounced near the Gurney flap. The pressure distribution becomes increasingly asymmetric with angle, notably beyond α = 8°.

As the angle of attack increases, the low-pressure region on the upper surface of the airfoil becomes more pronounced and the low-pressure region around the wing expands. This directly contributes to the increase in lift force. At α = 0°, a symmetric pressure distribution is observed, while at 4° and 8°, the negative pressure on the upper surface intensifies. At 12°, the flap-induced low-pressure region becomes larger, indicating the initial signs of flow separation. These contours demonstrate that the Gurney flap improves lift performance, particularly at higher angles of attack.

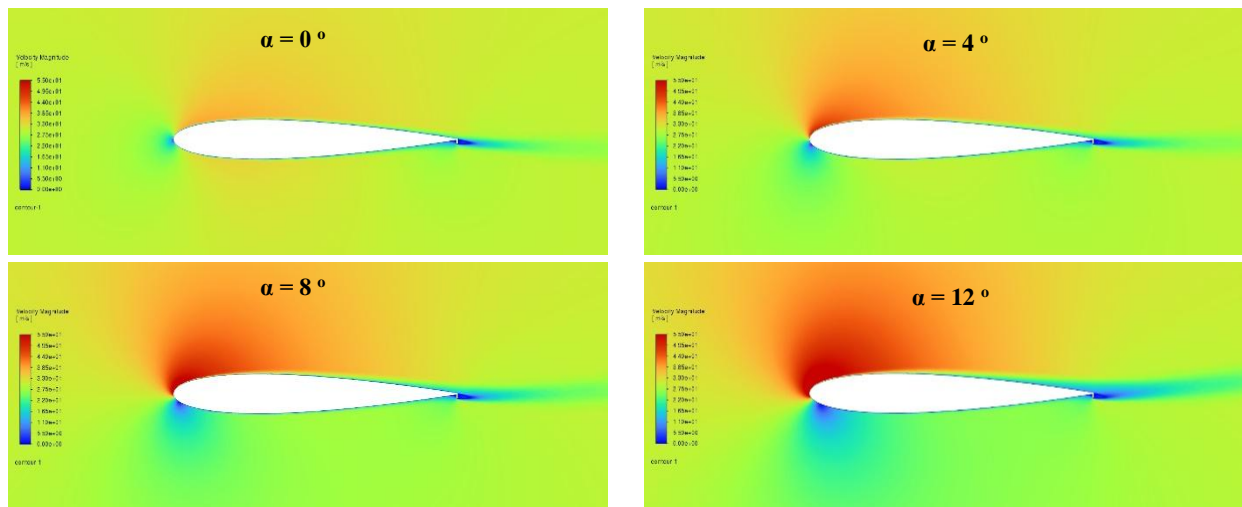


**Figure 5.** Velocity contours at α = 0°, 4°, 8° and 12°

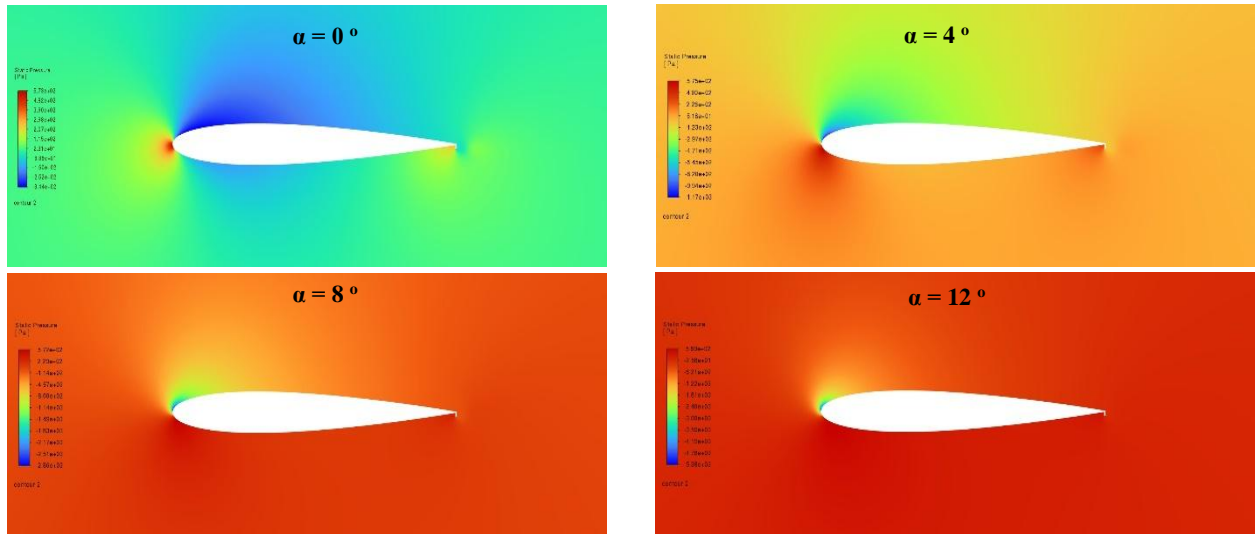


Figure 6. Static pressure contours at  $\alpha = 0^\circ, 4^\circ, 8^\circ,$  and  $12^\circ$

### 3.2. Variation of Lift and Drag Coefficients with Angle of Attack

To quantitatively assess the aerodynamic performance of the NACA 0012 airfoil equipped with a Gurney flap, three key aerodynamic parameters were evaluated: lift coefficient (CL), drag coefficient (CD), and lift-to-drag

ratio (CL/CD). These parameters provide insight into the effectiveness of each turbulence model in predicting aerodynamic forces at various angles of attack. The following figures (Figures 7–9) illustrate the numerical results obtained from each model, offering a comparative analysis against available experimental data.

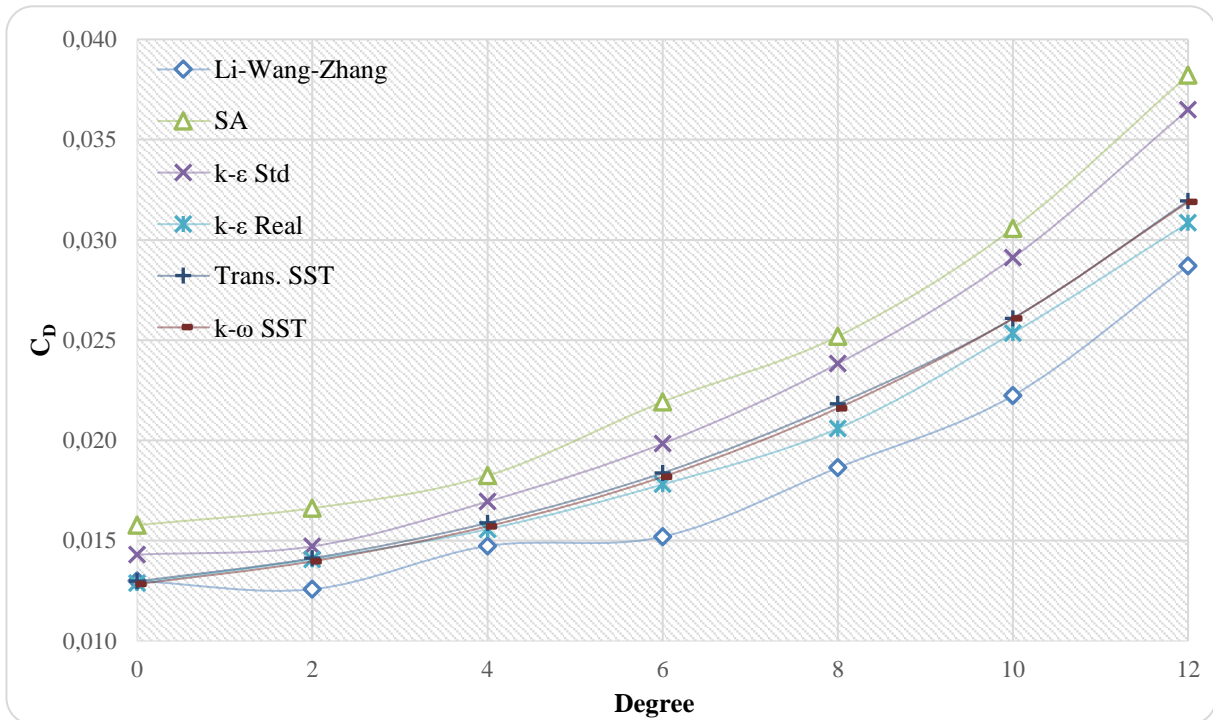


Figure 7. Drag coefficient ( $C_D$ ) vs. angle of attack for different turbulence models

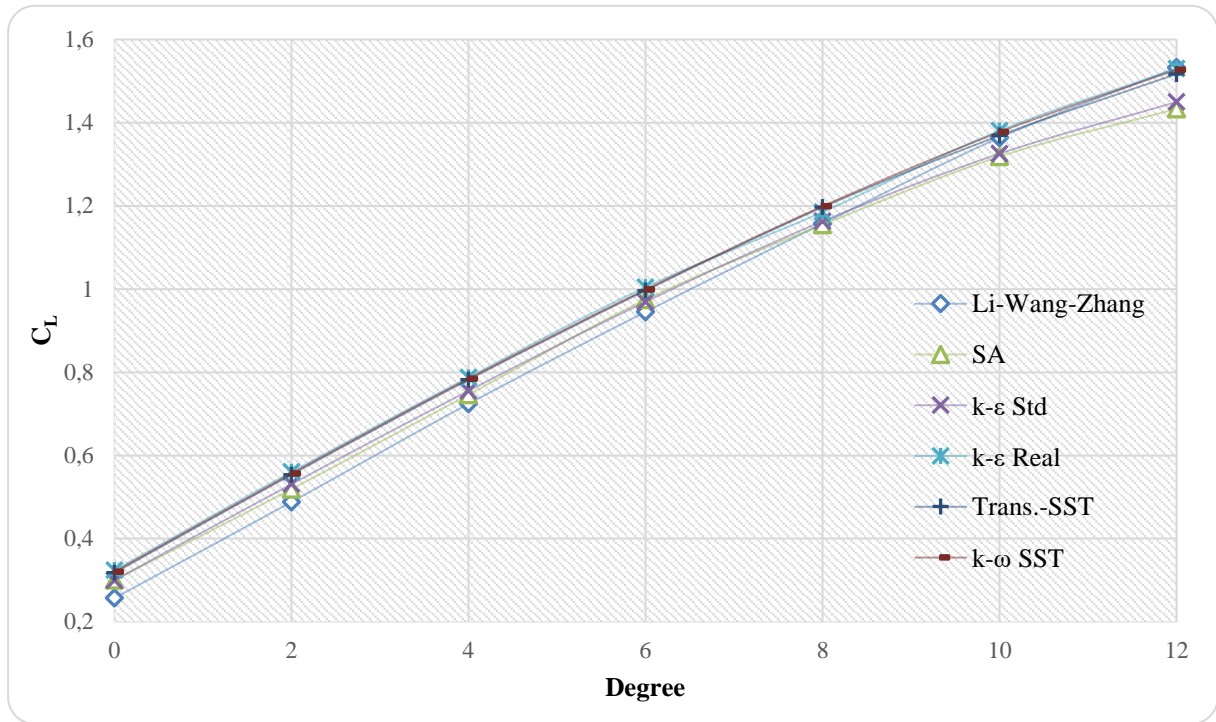


Figure 8. Lift coefficient ( $C_L$ ) vs. angle of attack for different turbulence models.

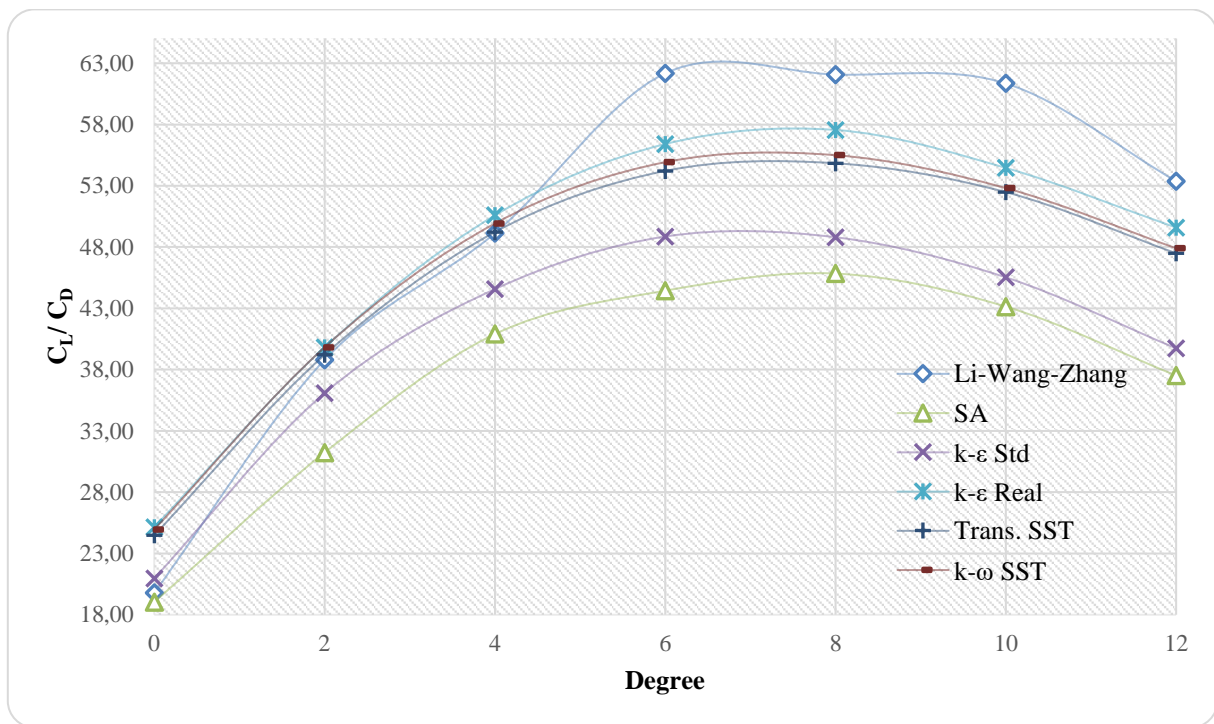


Figure 9. Lift-to-drag ratio ( $C_L/C_D$ ) vs. angle of attack for different turbulence model

In this study, the near-wall solution was performed using integration up to the wall (low-Re) for Spalart–Allmaras, SST  $k-\omega$ , and Transition SST, while the enhanced wall treatment (EWT) was used for  $k-\epsilon$  (Standard and Realizable). For all conditions,  $y^+$  values on the airfoil surface were reported statistically in the minimum and maximum values. For low-Re models, the target band was  $y^+ \approx 0.5-1$  (acceptable range 0.5–5), while for EWT,

a solution with a fine mesh of  $y^+ \lesssim 1$  was chosen. The results showed that  $y^+_{max} \lesssim 1$  for all models and angles, with typical values in the range of 0.01–0.71. Thus, both the low-Re and EWT approaches meet the validity criteria for near-wall resolution. According to Figure 9, it is demonstrated that the Transition SST model provides the highest aerodynamic efficiency from  $0^\circ$  to  $4^\circ$  while  $k-\epsilon$  Realizable model gives the best of that after 60 until

12o. The error rates obtained by comparing the CD and CL coefficients with experimental results for different turbulence models are presented in Table 3. According to Table 3, the minimum CD value was obtained as 0.14% at 0o for Transition SST while the maximum of that was

found as 44.25% at 6o for Spart-Allmaras. Besides, the minimum CL value was obtained as 0.16% at 12o for k Realizable while the maximum of that was found as 26.07% at 0o for same model.

**Table 3.** The error rates obtained by comparing CD and CL values with experimental results.

	Turbulence Models	Degree (°)	0	2	4	6	8	10	12
CD	Spalart-Allmaras	Errors (%)	21.47	32.13	23.80	44.25	35.14	37.47	33.11
	k-ε Std		10.11	16.98	15.00	30.54	27.84	30.95	27.11
	k-ε Realizable		0.81	11.82	5.65	17.16	10.48	14.04	7.47
	Transition SST		0.14	12.29	7.79	20.92	17.06	17.31	11.31
	k-ω		1.23	11.06	6.63	19.64	15.91	17.31	11.09
CL	Spalart-Allmaras		16.80	6.36	3.05	3.10	0.22	3.33	6.45
	k-ε Std		16.66	8.79	4.32	2.58	0.50	2.82	5.34
	k-ε Realizable		26.07	14.78	8.79	6.29	2.44	1.23	0.16
	Transition SST		23.61	13.47	7.99	5.43	3.42	0.35	0.97
	k-ω		24.59	14.00	8.35	5.69	3.63	0.99	0.31

In accordance with the reference article for flow separation, the variation of CL/CD to CL was given in

Figure 10. According to Figure 10, the flow separation has been seen after the CL value of 1.4.

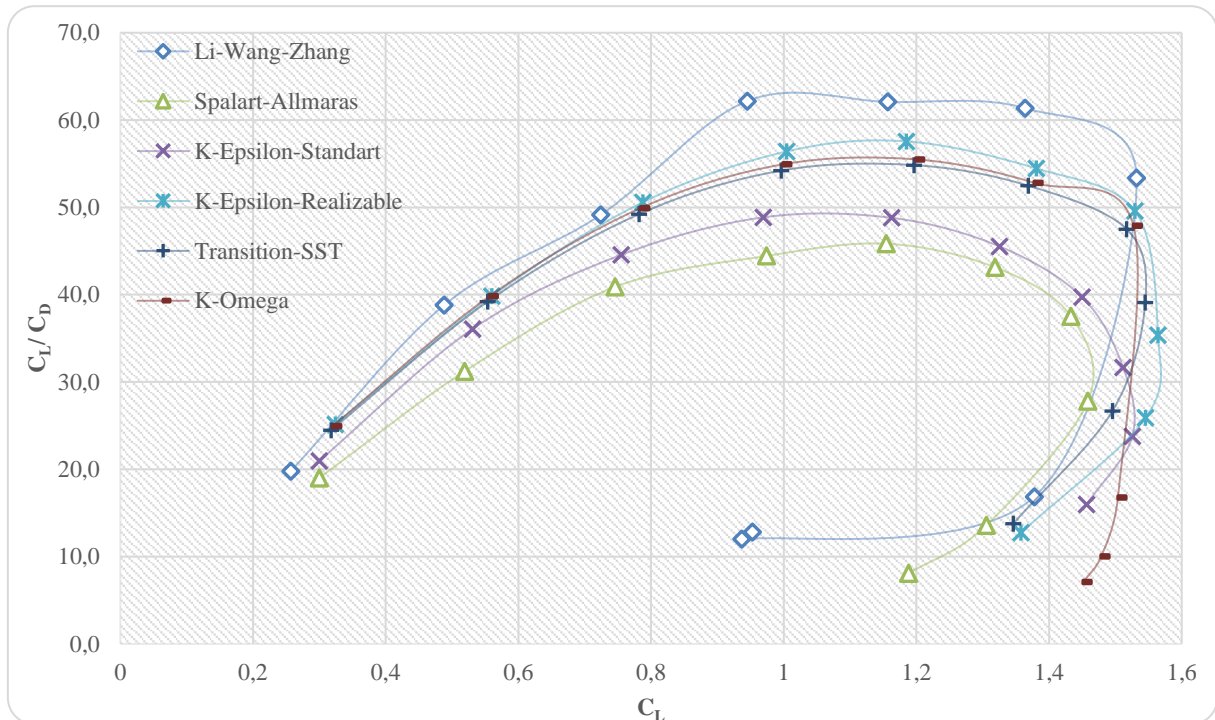


**Figure 10.** The variation of CL/CD to CL

#### 4. CONCLUSION

In this study, a computational investigation on the aerodynamic behavior of a NACA 0012 airfoil equipped with a 1.5% height Gurney flap was performed by utilizing various turbulence models in ANSYS Fluent. For this purpose, different five widely recognized turbulence models -Spalart-Allmaras, Standard k- $\epsilon$ , Realizable k- $\epsilon$ , SST k- $\omega$ , and Transition SST- were employed to assess their predictive accuracy under identical flow conditions. Firstly, the mesh independence study was performed, and 40,000 elements offers a reliable balance between computational cost and solution accuracy, thus strengthening the confidence in numerical comparisons. Compared to the other models, Transition SST and k- $\epsilon$  Realizable not only provided closer agreement with experimental data, but also consistently delivered more reliable predictions across a range of angles of attack. The strength of this model lies in its ability to accurately resolve transitional boundary layers and predict flow separation zones, which are critical in configurations incorporating passive flow control devices. The results of this study highlight the critical role of turbulence model selection for transitional aerodynamic flows, where accurate prediction of separation and wake dynamics is essential. Realizable k- $\epsilon$  and SST k- $\omega$  models provided reasonably accurate results in low to moderate angles of attack, though their performance declined in post-stall conditions. Standard k- $\epsilon$  and Spalart-Allmaras models overestimated drag and underestimated lift, particularly at  $\alpha \geq 10^\circ$ , likely due to limitations in modeling adverse pressure gradients and separation bubbles.

According to the errors, the minimum CD value was obtained as 0.14% at 0o for Transition SST while the maximum of that was found as 44.25% at 6o for Spart-Allmaras. Besides, the minimum CL value was obtained as 0.16% at 12o for k- $\epsilon$  Realizable while the maximum of that was found as 26.07% at 0o for same model. Moreover, it is demonstrated that the Transition SST model provides the highest aerodynamic efficiency from 0° to 4° while k- $\epsilon$  Realizable model gives the best of that after 6o until 12o. These findings highlight the importance of selecting a turbulence model tailored to the transitional flow behavior in CFD-based aerodynamic analyses. The Realizable k- $\epsilon$  model stands out due to its stable handling of separated-flow regions and its ability to produce CL and CD values in close agreement with experimental data. Moreover, it consistently provided reliable predictions across all evaluated angles of attack. Among the models evaluated in general view, the k- $\epsilon$  Realizable model is strongly recommended for future studies due to its superior capability in capturing both near-wall phenomena and wake dynamics with high accuracy. Its accurate resolution of laminar-to-turbulent transition and flow separation further reinforces its suitability for passive flow control simulations.

#### DECLARATION OF ETHICAL STANDARDS

The author(s) of this article declare that the materials and methods used in this study do not require ethical committee permission and/or legal-special permission.

#### AUTHORS' CONTRIBUTIONS

**Gökhan Çal:** Conceptualization, Geometry Design, CFD Simulations, Data Analysis, Writing Original Draft.  
**Halit Arat:** Supervision, Methodology Review, Validation, Writing – Review & Editing.

#### CONFLICT OF INTEREST

There is no conflict of interest in this study.

#### REFERENCES

- [1] R. H. Liebeck, "Design of subsonic airfoils for high lift," *Journal of Aircraft*, no. 9, vol. 15, pp. 547–561, (1978).
- [2] Y. Zhou, M. M. Alam, H. X. Yang, H. Guo and D. H. Wood, "Fluid forces on a very low Reynolds number airfoil and their prediction," *International Journal of Heat and Fluid Flow*, no. 1, vol. 32, pp. 329–339, (2011).
- [3] Y. Li, J. Wang and P. Zhang, "Effects of Gurney flaps on a NACA0012 airfoil," *Flow, Turbulence and Combustion*, no. 1, vol. 68, pp. 27–39, (2002).
- [4] M. Y. Iqbal, S. I. A. Shah and A. Hassan, "CFD analysis of NACA-0012 airfoil with various porous Gurney flap geometries," *Proceedings of the International Conference on Aerospace Science & Engineering (ICASE)*, (2019).
- [5] S. B. Pope, *Turbulent Flows*, Cambridge University Press, (2000).
- [6] S. M. Mousavi, J. Aminian, N. Shafiei and A. Dadvand, "Numerical simulation of subsonic turbulent flow over NACA0012 airfoil: Evaluation of turbulence models," *Sigma Journal of Engineering and Natural Sciences*, no. 1, vol. 35, pp. 133–155, (2017).
- [7] E. I. Basri, A. A. Basri and K. A. Ahmad, "Computational fluid dynamics analysis in biomimetics applications: A review from aerospace engineering perspective," *Biomimetics*, no. 3, vol. 8, (2023).
- [8] F. Z. Wang, I. L. Animasaun, T. Muhammad and S. S. Okoya, "Recent advancements in fluid dynamics: Drag reduction, lift generation, computational fluid dynamics, turbulence modelling, and multiphase flow," *Arabian Journal for Science and Engineering*, no. 8, vol. 49, pp. 10237–10249, (2024).
- [9] J. Priyadumkol et al., "CFD modelling of vertical-axis wind turbines using transient dynamic mesh towards lateral vortices capturing and Strouhal number," *Energy Conversion and Management: X*, (2025).
- [10] K. Karthikeyan and R. Harish, "CFD analysis of Gurney flap orientation and plasma actuation for turbulent flow control over NACA4412 airfoil," *Results in Engineering*, vol. 26, (2025).
- [11] S. Evran and S. Z. Yıldır, "Numerical and statistical aerodynamic performance analysis of NACA0009 and NACA4415 airfoils," *Politeknik Dergisi*, no. 3, vol. 27, pp. 849–856, (2024).
- [12] H. Gökçe, U. Küçük and İ. Şahin, "Effects of curvature and area distribution on S-shaped subsonic diffuser performance," *Mechanika*, no. 6, vol. 24, (2018).

- [13] K. M. Almohammadi, "Assessment of several modeling strategies on the prediction of lift-drag coefficients of a NACA0012 airfoil at a moderate Reynolds number," *Alexandria Engineering Journal*, no. 3, vol. 61, pp. 2242–2249, (2022).
- [14] S. Durmuş and A. Ulutaş, "Numerical analysis of NACA 6409 and Eppler 423 airfoils," *Politeknik Dergisi*, no. 1, vol. 26, pp. 39–47, (2023).
- [15] I. Celik, *Introductory Turbulence Modeling*, University of Alabama at Birmingham, (1999).
- [16] R. B. Langtry and F. R. Menter, "Correlation-based transition modeling for unstructured parallelized computational fluid dynamics codes," *AIAA Journal*, no. 12, vol. 47, pp. 2894–2906, (2009).
- [17] Y. F. Görgülü, M. A. Özgür and R. Köse, "CFD analysis of a NACA 0009 aerofoil at a low Reynolds number," *Politeknik Dergisi*, no. 3, vol. 24, pp. 1237–1242, (2021).
- [18] H. Soğukpınar, "Numerical investigation of aerodynamic characteristics," *Uludağ Üniversitesi Mühendislik Fakültesi Dergisi*, no. 1, vol. 22, pp. 169–178, (2017).
- [19] M. M. Yavuz, "Flow and mechanical characteristics of a modified NACA wing geometry," *Çukurova Üniversitesi Mühendislik Fakültesi Dergisi*, no. 3, vol. 36, pp. 815–825, (2021).
- [20] D.-H. Kim and J.-W. Chang, "Low-Reynolds-number effect on the aerodynamic characteristics of a pitching NACA0012 airfoil," *Aerospace Science and Technology*, no. 1, vol. 32, pp. 162–168, (2014).
- [21] G. Çal and H. Arat, "Aerodynamic analysis of the NACA0012 wing profile for different turbulence models," *Proceedings of the International Istanbul Scientific Research Congress*, pp. 688–694, (2025).
- [22] İ. Göv and M. H. Doğru, "Aerodynamic optimization of NACA 0012 airfoil," *The International Journal of Energy & Engineering Sciences*, no. 2, vol. 5, pp. 146–155, (2020).
- [23] A. İ. Gölcük and M. Erbaş, "Düşük Reynolds sayılarında NACA 0012 kanat profilinin k- $\omega$  SST türbülans modeli kullanılarak hesaplamalı akışkanlar dinamiği ile modellenmesi," *Ulusal Havacılık ve Uzay Konferansı Bildiriler Kitabı*, (2020).